A Fourth Order FDFD Approach for the Analysis of Sectorial Elliptic Waveguides

Alessandro Fanti, Luisa Deias, Giovanni Andrea Casula, and Giorgio Montisci

Department of Electrical and Electronic Engineering
University of Cagliari, 09123, Piazza d'Armi, Cagliari, Italy
{alessandro.fanti, luisa.deias, a.casula, giorgiom}@diee.unica.it

Abstract **─** We present a fourth order frequency domain finite difference approach (FDFD) in curvilinear coordinates for the computation of the modes of sectorial and ridged elliptic waveguides. The use of an elliptic mesh allows to avoid usual the staircase approximations of the boundary, providing a very effective and accurate procedure.

Index Terms **─** Cutoff frequency, elliptical ridged waveguide analysis, finite difference frequency domain, microwave components, microwave filters, ridged waveguides, waveguide modes.

I. INTRODUCTION

Application of sectorial and ridged circular and elliptic waveguides [1] can be found in many components like filters, matching networks, orthomode transducers, polarizers and circulators that are widely used in satellite and terrestrial communication systems [2-6]. Low-cost design, small size, and optimal performance of these components are essential to satisfy today's stringent payload requirements. Analysis and design of such structures requires the solution of waveguide problems, which can be faced both with general-purpose software and with specialized numerical techniques, such as methods of moments (MoM) [7-9] and mode-matching (MM) [10-11]. However, MM requires an accurate knowledge of the waveguide modes to be implemented. The same type of information is also required in the analysis, using MoM, of thick-walled apertures [12] and slots [13-14]. Indeed, these apertures can be considered as stub waveguides, and the modes of these guides are the natural basis functions for the MoM [15].

Apart from some simple geometries, where analytical evaluation of such modes is possible, the mode computation cannot be done in closed form (or the closed-form solution is unsuitable for effective use). In particular, for a circular waveguide, the analytic computation of the modes is simple, since the mode distribution can be expressed in terms of Bessel functions and the eigenvalues are the zeroes of these functions, which are well-known [16]. An analytical, closed form solution exists also for elliptic waveguides and has been found by Chu [17] since the 30's. Unfortunately, the field distribution is described by the Mathieu functions [18], whose numerical evaluation is very cumbersome. The best approach seems the expansion of those functions in a series of (more tractable) Bessel functions [19]. These series are not quickly converging, so the evaluation of these series are computationally heavy, above all when a high accuracy is required. In the literature, there are many different approximate or numerical techniques for the solution the Helmholtz equation. In particular, the frequency-domain finite-difference approach (FDFD) [20], namely the direct discretization of the differential eigenvalue problem is the simplest strategy however, and can be applied to both scalar [21-22] and vector [23] problems. Despite of its simplicity, in many cases it is accurate and computationally effective, too, since at variance of, e.g., [24] it leads to matrices which are highly sparse. However, accuracy or effectiveness (or both) are lost for guides with curved boundary, since the most popular FDFD implementation amount to replace the correct boundary geometry with a staircase approximation a solution which strongly affects the accuracy or the computational load (or both). Nevertheless, it is still adopted also in sophisticated numerical techniques [25].

Submitted On: June 30, 2014
Accepted On: December 11, 2014

Aim of this work is to devise a FDFD approach for sectorial (SEW) and ridged (REW) homogeneous elliptic waveguides, tailored to the structure, but as simple as the standard one in the formulation. Use of a suitable elliptical grid (which perfectly fits the waveguide boundary) allows to evaluate the SEW and REW modes with the required accuracy using order of magnitude less sampling points than the standard approach. For each grid point, a fourth-order Taylor approximations allow to replace the continuous eigenfunction problem with a discrete one. This work is therefore an extension of work presented in [26], where a second-order approximation has been used.

The proposed approach has been validated by comparison with some analytical results found in literature [27].

II. DESCRIPTION OF TECNIQUE

Let us consider an empty elliptic waveguide. Both TE and TM modes can be found from a suitable scalar eigenfunction, solution of the Helmholtz equation:

$$\nabla_t^2 \phi + k_t^2 \phi = 0 \,, \tag{1}$$

with the boundary conditions (BC):

$$\begin{aligned} &\frac{\partial \phi}{\partial n} = 0 \quad (TE \text{ modes}) \\ &\phi = 0 \qquad (TM \text{ modes}) \end{aligned} \,, \tag{2}$$

at the boundary of the ridged waveguide. Both the equation (1) and the BC (2) can be replaced by a discretized version, looking for the eigenvalues and eigenfunction defined on a suitable set of sampling points, and therefore replacing derivatives with finite approximations. The standard solution is to use a rectangular set of sampling points [22], but this forces to replace the curved boundary with a staircase approximation. This approximation results in a low accuracy (using a course grid), or in a heavy computational load (using a very fine grid). Since we are interested in elliptic boundaries, our propose here is to select a set of sampling points located on the elliptic coordinates framework (see Fig. 1).

We choose a regular spacing on the elliptic coordinate lines, with step $\Delta u, \Delta v$. Letting $\phi_{pq} = \phi\left(p\Delta u, q\Delta v\right)$, the eigenvalues equation (1) should be:

$$\frac{1}{a^2\left(\sinh^2 p\Delta u + \sin^2 q\Delta v\right)} \cdot \left[\frac{\partial^2 \phi}{\partial u^2} + \frac{\partial^2 \phi}{\partial v^2}\right]_{pq} = -k_t^2 \phi_{pq} \,. \tag{3}$$

For each internal point P (see Fig. 2) is simpler to discretize the term in brackets (3) using a fourth-order Taylor expansion:

$$\begin{aligned} \phi_B = \phi_P &+ \left.\frac{\partial \phi}{\partial u}\right|_P \cdot (-\Delta u) + \frac{1}{2}\left.\frac{\partial^2 \phi}{\partial u^2}\right|_P \cdot (-\Delta u)^2 + \\ &+ \frac{1}{6}\left.\frac{\partial^3 \phi}{\partial u^3}\right|_P \cdot (-\Delta u)^3 + \frac{1}{24}\left.\frac{\partial^4 \phi}{\partial u^4}\right|_P \cdot (-\Delta u)^4 \end{aligned} \,, \tag{4}$$

$$\begin{aligned} \phi_N = \phi_P &+ \left.\frac{\partial \phi}{\partial u}\right|_P \cdot (-2\Delta u) + \frac{1}{2}\left.\frac{\partial^2 \phi}{\partial u^2}\right|_P \cdot (-2\Delta u)^2 + \\ &+ \frac{1}{6}\left.\frac{\partial^3 \phi}{\partial u^3}\right|_P \cdot (-2\Delta u)^3 + \frac{1}{24}\left.\frac{\partial^4 \phi}{\partial u^4}\right|_P \cdot (-2\Delta u)^4 \end{aligned} \,, \tag{5}$$

$$\begin{aligned} \phi_D = \phi_P &+ \left.\frac{\partial \phi}{\partial u}\right|_P \cdot (\Delta u) + \frac{1}{2}\left.\frac{\partial^2 \phi}{\partial u^2}\right|_P \cdot (\Delta u)^2 + \\ &+ \frac{1}{6}\left.\frac{\partial^3 \phi}{\partial u^3}\right|_P \cdot (\Delta u)^3 + \frac{1}{24}\left.\frac{\partial^4 \phi}{\partial u^4}\right|_P \cdot (\Delta u)^4 \end{aligned} \,, \tag{6}$$

$$\begin{aligned} \phi_Q = \phi_P &+ \left.\frac{\partial \phi}{\partial u}\right|_P \cdot (2\Delta u) + \frac{1}{2}\left.\frac{\partial^2 \phi}{\partial u^2}\right|_P \cdot (2\Delta u)^2 + \\ &+ \frac{1}{6}\left.\frac{\partial^3 \phi}{\partial u^3}\right|_P \cdot (2\Delta u)^3 + \frac{1}{24}\left.\frac{\partial^4 \phi}{\partial u^4}\right|_P \cdot (2\Delta u)^4 \end{aligned} \,. \tag{7}$$

By combining the four last equations we find:

$$\left.\frac{\partial^2 \phi}{\partial u^2}\right|_P = \frac{1}{12\Delta u^2} \cdot \left(16\phi_B + 16\phi_D - \phi_N - \phi_Q - 30\phi_P\right). \tag{8}$$

Likely in v direction:

$$\left.\frac{\partial^2 \phi}{\partial v^2}\right|_P = \frac{1}{\Delta v^2} \cdot \left(16\phi_H + 16\phi_G - \phi_A - \phi_C - 30\phi_P\right). \tag{9}$$

Expression (8,9) are the substituted in the term in brackets (3) to get:

$$\begin{aligned} &\left[\frac{\partial^2 \phi}{\partial u^2} + \frac{\partial^2 \phi}{\partial v^2}\right] = \\ &\frac{16}{12\Delta v^2} \cdot \phi_H + \frac{16}{12\Delta v^2} \cdot \phi_G - \frac{1}{12\Delta v^2} \cdot \phi_A - \frac{1}{12\Delta v^2} \cdot \phi_C \\ &\frac{16}{12\Delta u^2} \cdot \phi_B + \frac{16}{12\Delta u^2} \cdot \phi_D - \frac{1}{12\Delta u^2} \cdot \phi_N - \frac{1}{12\Delta u^2} \cdot \phi_Q \\ &-\frac{30}{12}\left(\frac{1}{\Delta u^2} + \frac{1}{\Delta v^2}\right) \cdot \phi_P \end{aligned} \,, \tag{10}$$

which easily leads to the FDFD approximation of (1).

Equation (10) cannot be used for the two foci, for points between them and for external points. For a point P lying on the segment joining the two foci we can integrate (1):

$$\int \nabla_t^2 \phi dS = -k_t^2 \int \phi dS\theta \, , \tag{11}$$

and apply the Gauss theorem to obtain:

$$\int_{\Gamma_F} \frac{\partial \phi}{\partial n} \cdot dl = -k_t^2 \int_{S_F} \phi dS, \tag{12}$$

wherein S_F is the cell surface, and Γ_F is the cell boundary.

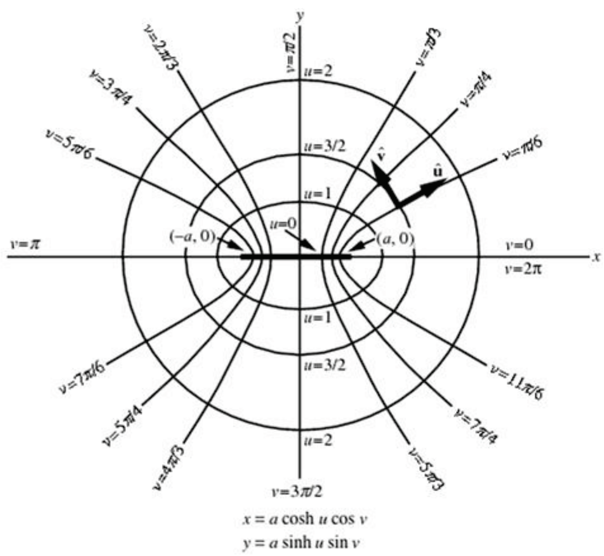

Fig. 1. Geometry of the elliptic coordinates [28].

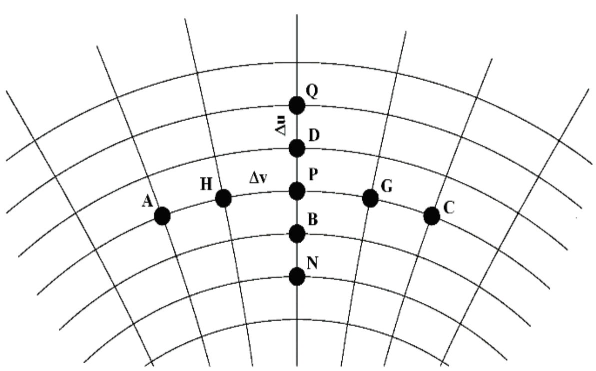

Fig. 2. Internal point of the elliptic coordinates grid TE and TM.

In the elliptic grid used for a SEW or REW, we have two types of boundary points: the radial ones (P in Fig. 3 (a)) and the angular ones (P in Fig. 3 (b)).

The TE boundary condition can be enforced in the same way for both types of boundary points, so we describe it only for an elliptic one (Fig. 3). The boundary point X in Fig. 2 (a) is not a discretization point. Therefore, use of the Taylor expansion would require an extrapolation of $\phi(u)$ outside the sampling region, using either ϕ_X to enforce the boundary condition $\frac{\partial \phi}{\partial n} = 0$.

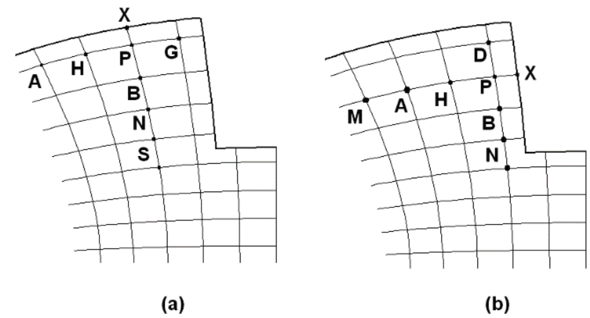

Fig. 3. (a) Geometry pertinent to the first type of boundary point P, and (b) geometry pertinent to the second type of boundary point P.

Let us consider an edge point P (Fig. 3 (a)), we can write the second derivative in u, as:

$$\frac{\partial^2 \phi}{\partial u^2} \cong \sum_{i=B}^{np} A_i \left(\phi_i - \phi_P\right) = \\ = \left[B_1 \left.\frac{\partial \phi}{\partial u}\right|_P + B_2 \left.\frac{\partial^2 \phi}{\partial u^2}\right|_P + B_3 \left.\frac{\partial^3 \phi}{\partial u^3}\right|_P + B_4 \left.\frac{\partial^4 \phi}{\partial u^4}\right|_P \right], \tag{13}$$

where:

$$B_1 = \sum_{i=1}^{np} A_i \cdot \Delta u_i \, , \quad B_2 = \sum_{i=1}^{np} A_i \cdot \Delta u_i^2 \, ,$$

$$B_3 = \sum_{i=1}^{np} A_i \cdot \Delta u_i^3 \, , \quad B_4 = \sum_{i=1}^{np} A_i \cdot \Delta u_i^4 \, ,$$

are linear combinations of the unknown coefficient A_i, and $np = 3$ is the number of the points used in the expression $(i = B, N, S)$.

Now can be expressed $\partial \phi / \partial u = 0$ using Taylor series:

$$\left.\frac{\partial \phi}{\partial u}\right|_X \simeq \left.\frac{\partial \phi}{\partial u}\right|_P + \left.\frac{\partial^2 \phi}{\partial u^2}\right|_P \cdot \left(\frac{\Delta u}{2}\right) + \\ + \frac{1}{2} \left.\frac{\partial^3 \phi}{\partial u^3}\right|_P \cdot \left(\frac{\Delta u}{2}\right)^2 + \frac{1}{6} \left.\frac{\partial^4 \phi}{\partial u^4}\right|_P \cdot \left(\frac{\Delta u}{2}\right)^3 = 0, \tag{14}$$

which can be solved for $\left.\frac{\partial \phi}{\partial u}\right|_P$. Its expression is used to and can be used for replace of the terms in the bracket on the r.h.s. of equation (13):

$$\left(B_2 - B_1\frac{\Delta u}{2}\right)\cdot\left.\frac{\partial^2\phi}{\partial u^2}\right|_P + \left(B_3 - B_1\frac{\Delta u^2}{8}\right)\cdot\left.\frac{\partial^3\phi}{\partial u^3}\right|_P + \\ +\left(B_4 - B_1\frac{\Delta u^3}{48}\right)\left.\frac{\partial^4\phi}{\partial u^4}\right|_P . \quad (15)$$

Eq. (15) is an approximation of $\frac{\partial^2\phi}{\partial u^2}$ if:

$B_2 - B_1\frac{\Delta u}{2} = 1$, $B_3 - B_1\frac{\Delta u^2}{8} = 0$, $B_4 - B_1\frac{\Delta u^3}{48} = 0$, and coefficients A_i are given by the solution of the linear system (15) so (8) is replaced by:

$$\left.\frac{\partial^2\phi}{\partial u^2}\right|_P = \frac{1}{24\Delta u^2}\cdot\left(21\phi_B + 3\phi_N - \phi_S - 23\phi_P\right). \quad (16)$$

In the same way, we can replace (9) by:

$$\left.\frac{\partial^2\phi}{\partial v^2}\right|_P = \frac{1}{264\Delta v^2}\cdot\left(357\phi_H + 335\phi_G - 23\phi_A - 792\phi_P\right), \quad (17)$$

and the equation (10) becomes:

$$\frac{21}{24\Delta u^2}\phi_B + \frac{3}{24\Delta u^2}\phi_N - \frac{1}{24\Delta u^2}\phi_S + \\ \frac{357}{264\Delta v^2}\phi_H + \frac{335}{264\Delta v^2}\phi_G - \frac{23}{264\Delta v^2}\phi_A + . \\ -\left(\frac{23}{24\Delta u^2} + \frac{792}{264\Delta v^2}\right)\phi_P \cong -k_t^2\phi_P^2 \quad (18)$$

A significant advantage of the present approach is that TM modes can be computed on the same TE grid, at variance of the standard approach [22], which calls for two different sets of sampling points, to cope with the different BC (2). To get the TM modes on the same grid, we express the potential in X through a Taylor approximation:

$$\phi_X = \phi_P + \left.\frac{\partial\phi}{\partial u}\right|_P\cdot\left(\frac{\Delta u}{2}\right) + \frac{1}{2}\left.\frac{\partial^2\phi}{\partial u^2}\right|_P\cdot\left(\frac{\Delta u}{2}\right)^2 + \\ +\frac{1}{6}\left.\frac{\partial^3\phi}{\partial u^3}\right|_P\cdot\left(\frac{\Delta u}{2}\right)^3 + \frac{1}{24}\left.\frac{\partial^4\phi}{\partial u^4}\right|_P\cdot\left(\frac{\Delta u}{2}\right)^4 , \quad (19)$$

and set $\phi_X = 0$. By adding the last equation with (13) and solving the linear system (8) we get:

$$\left.\frac{\partial^2\phi}{\partial u^2}\right|_P = \frac{7}{3\Delta u^2}\phi_B - \frac{2}{5\Delta u^2}\phi_N + \frac{1}{21\Delta u^2}\phi_S - \frac{16}{3\Delta u^2}\phi_P . \quad (20)$$

Likely in v direction:

$$\left.\frac{\partial^2\phi}{\partial v^2}\right|_P = \frac{1}{3\Delta v^2}\phi_G + \frac{5}{3\Delta v^2}\phi_H - \frac{2}{15\Delta v^2}\phi_A - \frac{4}{\Delta v^2}\phi_P, \quad (21)$$

combining the equations (20) and (21) into (10) we find the final expression:

$$\frac{7}{3\Delta u^2}\phi_B - \frac{2}{5\Delta u^2}\phi_N + \frac{1}{21\Delta u^2}\phi_S + \\ \frac{1}{3\Delta v^2}\phi_G + \frac{5}{3\Delta v^2}\phi_H - \frac{2}{15\Delta v^2}\phi_A + . \\ -\left(\frac{4}{\Delta v^2} + \frac{16}{3\Delta u^2}\right)\phi_P \cong -k_t^2\phi_P^2 \quad (22)$$

In the point in Fig. 3 (b), we use the same procedure to calculate the approximation of laplace operator for TE and TM modes.

III. RESULTS

The fourth-order FDFD for elliptic ridge waveguide described in the previous sections has been extensively validated, to evaluate its accuracy and effectiveness. In the simulations presented in this section, we will consider first a sector of elliptic ridged waveguide (see Fig. 4) and then a ridged sector. All dimensions have been normalized to the minor semi-axis of the ellipse.

Our FDFD procedure has been assessed against the analytical results of [27]. The resulting eigenvalue problem has been solved using standard MATLAB routines, on a PC with two Intel Xeon E5504 CPUs@2.00 GHz, 48 GB RAM, OS: MS Windows 7 Professional.

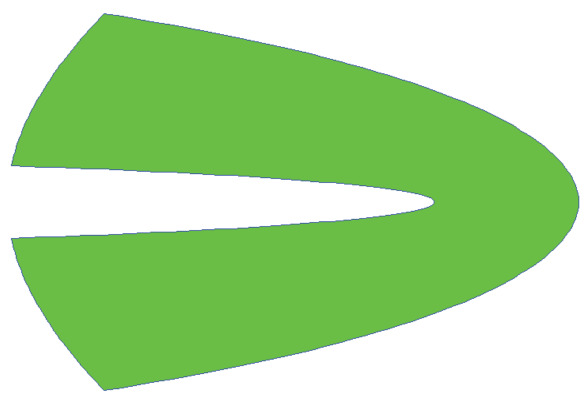

Fig. 4. Elliptic sectorial guide with $u_1 = 0.1$, $u_2 = 0.5$, and $v_1 = -50°$, $v_2 = 50°$.

The main results of our validation are collected in the next tables $u \in (u_1, u_2)$, $v \in (v_1, v_2)$. From them it appears that our FDFD approach is able to give a very high accuracy, with a difference (with respect to the accurate data of [27]), which is smaller than 0.02% in most cases.

The computation time of the FDFD approach is the sum of the matrix filling time and the time needed to extract eigenvalue and eigenvectors of the sparse matrix. For example, for a grid with $\Delta u = 0.0040$, $\Delta v = 0.0009$ and 1010000 points, the filling matrix time is 2,07 sec and the time to extract eigenvalue and eigenvectors is 93.02 sec.

Table 1: Relative error on normalized TE cut-off wavelengths, with respect to [27], for the guide of Fig. 4, $\Delta u = 0.0078$, $\Delta v = 0.01755$

TE	λ_C/a [27]	λ_C/a Our Code	Relative Error %
1	2.656401	2.656343	0.0022
2	6.836981	6.835793	0.0174
3	9.544562	9.540887	0.0385

Table 2: Relative error on normalized TM cut-off wavelengths, with respect to [27], for the guide of Fig. 4, $\Delta u = 0.0078$, $\Delta v = 0.01755$

TM	λ_C/a [27]	λ_C/a Our Code	Relative Error %
1	14.283213	14.280411	0.0196
2	14.299466	14.297190	0.0159
3	19.561598	19.545863	0.0804

Table 3: Relative error on normalized TE cut-off wavelengths, with respect to [27], for the guide of Fig. 4, $\Delta u = 0.004$, $\Delta v = 0.0017$

TE	λ_C/a [27]	λ_C/a Our Code	Relative Error %
1	2.656401	2.656366	0.0013
2	6.836981	6.836941	0.0006
3	9.544562	9.544720	0.0017

Table 4: Relative error on normalized TM cut-off wavelengths, with respect to [27], for the guide of Fig. 4, $\Delta u = 0.004$, $\Delta v = 0.0017$

TM	λ_C/a [27]	λ_C/a Our Code	Relative Error %
1	14.283213	14.283476	0.0018
2	14.299466	14.300252	0.0055
3	19.561598	19.558674	0.0150

In Fig. 5, left, we show the potential eigenfunctions for the first three TE modes (corresponding to the data of Table 1).

In order to show the flexibility of our approach, a different, ridged, sector has been considered. Only the eigenfunctions has been reported, since no analytic data is available. In Figs. 6 and 7 report a convergence analysis, with respect to the side of the discretization step. It appears that a fourfold reduction in Δv allows an accuracy increase of more than an order of magnitude. The behavior respect to Δu is different, since the structure is quite slender.

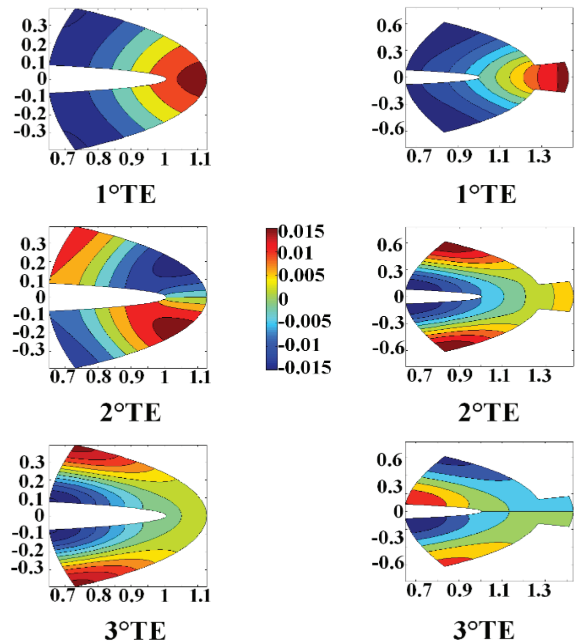

Fig. 5. Lowest-order eigenvectors for the examples presented. Left: structure of Fig. 4. Right: ridged sectorial guide with $u_1 = 0.1$, $u_2 = 0.74$, $v_1 = -50°$, $v_2 = 50°$, and $u_3 = 0.1$, $u_4 = 0.9$, $v_3 = -10°$, $v_4 = 10°$.

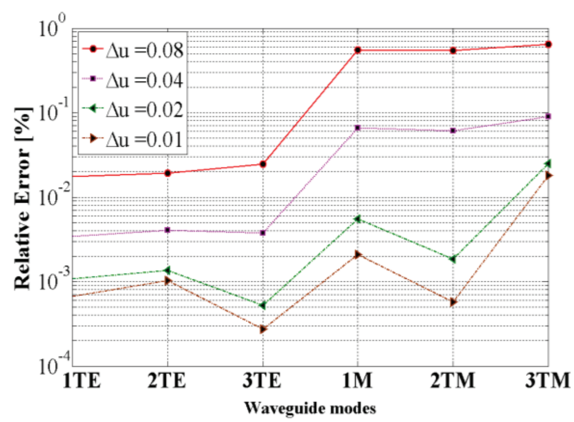

Fig. 6. Relative error on the cut-off frequency of the first modes of an elliptic sector waveguide with $\Delta v = 0.0017$.

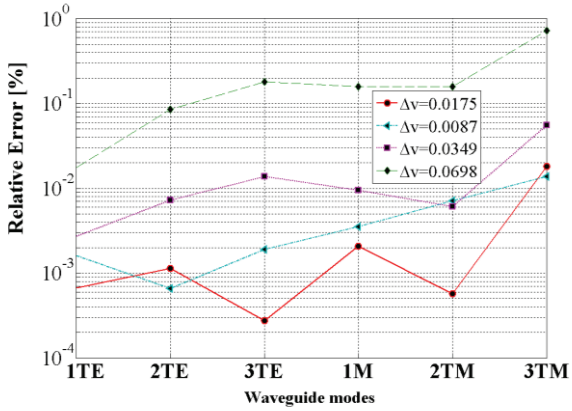

Fig. 7. Relative error on the cut-off frequency of the first modes of an elliptic sector waveguide with $\Delta u = 0.01$.

Finally in Fig. 8, we compare the present fourth-order FDFD with a lively second order one, with different discretization steps. Figure 8 shows clearly that the accuracy of a fourth order approach can be reached using a second-order one, but with at least four times the discretization points, and therefore a computational load larger by nurse than an order of magnitude. Therefore, the proposed use of a fourth-order approximation is a significant improvement with respect to [26].

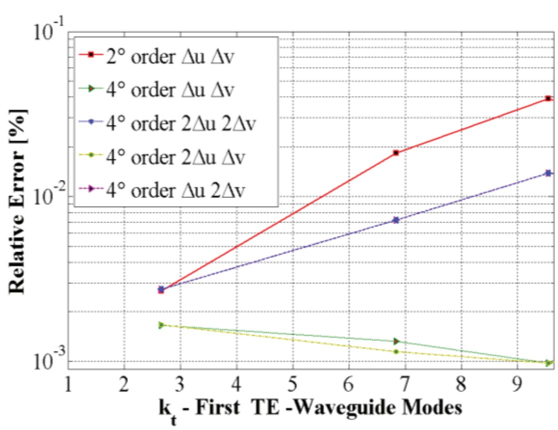

Fig. 8. Comparison of fourth and second order FDFD for the comparison of the k_t of the first TE modes for the structure of Fig. 4, for different discretization steps, $(\Delta u = 0.004, \Delta v = 0.0017)$.

IV. CONCLUSION

An approach to the FDFD computation of modes of an elliptic ridged waveguide has been presented. We describe here a fourth order finite difference frequency domain approach to the mode computation for both TE and TM modes. An elliptic mesh has been used in order to avoid staircase approximations of the boundary. The presented results show both the flexibility of the method, as well as its simplicity for the computation for TE and TM modes in an elliptic ridged waveguide.

ACKNOWLEDGMENT

Alessandro Fanti gratefully acknowledges Sardinia Regional Government for the financial support of her Post Doc fellowship (P.O.R. Sardegna F.S.E. Operational Programme of the Autonomous Region of Sardinia, European Social Fund 2007-2013 - Axis IV Human Resources, Objective l.3, Line of Activity l.3.1.).

REFERENCES

[1] A. A. El-Sherbiny, "Cutoff wavelengths of ridged, circular, and elliptic guides," *IEEE Trans. Microwave Theory Tech.*, vol. 21, pp. 7-12, Jan. 1973.

[2] A. E. Williams and A. E. Atia, "Dual-mode canonical waveguide filters," *IEEE Transactions on Microwave Theory & Techniques*, vol. 25, no. 12, pp. 1021-1026, Dec. 1977.

[3] R. Behe and P. Brachat, "Compact duplexer-polarizer with semicircular waveguide," *IEEE Trans. Antennas Propagat.*, vol. 39, pp. 1222-1224, Aug. 1991.

[4] B. V. de la Filolie and R. Vahldieck, "Coaxial and circular waveguide band-pass filters using printed metal inserts," *IEEE MTT-S Int. Microwave Symp. Dig.*, pp. 905-908, 1992.

[5] J. Huang, R. Vahldieck, and H. Jin, "Computer-aided design of circular ridged waveguide evanescent-mode bandpass filters using the FDTLM method," *IEEE MTT-S Int. Microwave Symp. Dig.*, pp. 459-462, 1993.

[6] U. Balaji and R. Vahldieck, "Mode matching analysis of circular-ridged waveguide discontinuities," *IEEE Trans. Microwave Theory Tech.*, vol. 46, pp. 191-195, Feb. 1998.

[7] G. Mazzarella and G. Montisci, "Wideband equivalent circuit of a centered-inclined waveguide slot coupler," *Journal of Electromagnetic Waves and Applications*, vol.

14, pp. 133-151, 2000.

[8] H. P. Zhao and Z. X. Shen, "Efficient modeling of three-dimensional reverberation chambers using hybrid discrete singular convolution-method of moments," *IEEE Transactions on Antennas and Propagation*, vol. 59, issue: 8, pp. 2943-2953, Aug. 2011.

[9] G. Mazzarella and G. Montisci, "Accurate characterization of the interaction between coupling slots and waveguide bends in waveguide slot arrays," *IEEE Trans. Microw. Theory Tech.*, vol. MTT-48, pp. 1154-1157, Sept. 2000.

[10] L. Prkna, M. Hubalek, and J. Ctyroky, "Vectorial eigenmode solver for bent waveguides based on mode matching," *Photonics Technology Letters, IEEE*, vol. 16, issue (9), pp. 2057-2059, Sept. 2004.

[11] M. Mongiardo and C. Tomassoni, "Modal analysis of discontinuities between elliptical waveguides," *IEEE Trans. Microw. Theory Tech*., vol. MTT-48, pp. 597-605, Apr. 2000.

[12] G. Mazzarella and G. Montisci, "A rigorous analysis of dielectric-covered narrow longitudinal shunt slots with finite wall thickness," *Electromagnetics*, vol. 19, pp. 407-418, 1999.

[13] G. Montisci, M. Musa, and G. Mazzarella, "Waveguide slot antennas for circularly polarized radiated field," *IEEE Transactions on Antennas and Propagation*, vol. 52, pp. 619-623, 2004.

[14] S. R. Rengarajan, "Compound radiating slot in a broad wall of a rectangular waveguide," *IEEE Transactions on Antennas Propagation*, vol. 37, pp. 1116-1124, 1989.

[15] G. Montisci, G. Mazzarella, and G. A. Casula, "Effective analysis of a waveguide longitudinal slot with cavity," *IEEE Transactions on Antennas and Propagation*, vol. 60, pp. 3104-3110, 2012.

[16] M. Abramowitz and I. A. Stegun, *Handbook of Mathematical Functions*, 1972: National Bureau of Standards.

[17] L. J. Chu, "Electromagnetic waves in elliptic hollow pipes of metal," *J. Appl. Phys.*, vol. 9, 583-591, 1938.

[18] N. Marcuvitz, *Waveguide Handbook*, Peregrinus, London, 1986.

[19] J. G. Kretzschmar, "Wave propagation in hollow conducting elliptical waveguides," *IEEE Trans. Microwave Theory Techniques*, vol. 18, pp. 547-554, 1970.

[20] T. Weiland, "Three dimensional resonator mode computation by finite difference method," *IEEE Trans. Magn*., vol. 21, pp. 2340-2343, 1985.

[21] A. Fanti, G. Mazzarella, G. Montisci, and G. A. Casula, "Computation of the modes of elliptic waveguides with a curvilinear 2D frequency-domain finite-difference approach," *Progress In Electromagnetics Research M*, vol. 26, 69-84, 2012.

[22] A. Fanti and G. Mazzarella, "A finite difference polar-cartesian grid approach for mode computation in rounded-end waveguides," *ACES Journal*, vol. 26, no. 9, Sept. 2011.

[23] A. Fanti, G. Montisci, G. Mazzarella, and G. A. Casula, "VFD approach to the computation TE and TM modes in elliptic waveguide on TM grid," *ACES Journal*, vol. 28, no. 12, Dec. 2013.

[24] Y. Shunchuan, C. Zhizhang, Y. Yiqiang, and S. Ponomarenko, "A divergence-free meshless method based on the vector basis function for transient electromagnetic analysis," *Microwave Theory and Techniques, IEEE Transactions on*, vol. 62, issue 7, pp. 1409-1416, Jul. 2014.

[25] M. Chai, T. Xiao, G. Zhao, and Q. H. Liu, "A hybrid PSTD/ADI-CFDTD method for mixed-scale electromagnetic problems," *IEEE Transactions on Antennas and Propagation*, vol. 55, issue 5, pp. 1398-1406, 2007.

[26] A. Fanti and L. Deias, "A new approach the analysis of sectorial elliptic waveguides," *30th International Review of Progress in Applied Computational Electromagnetics*, Jacksonville, Florida, Mar. 23-27, 2014.

[27] G. Amendola, G. Di Massa, and G. Angiulli, "Elliptic-hyperbolical waveguides," *Journal of Electromagnetic Waves and Applications*, vol. 14, issue 11, pp. 1473-1487, 2000.

[28] http://mathworld.wolfram.com/EllipticCylindricalCoordinates.html.

Alessandro Fanti received the Laurea degree in Electronic Engineering and Ph.D. degree in Electronic Engineering and Computer Science from the University of Cagliari, Cagliari, Italy, in 2006 and 2012, respectively. He currently holds a Post-Doc scholarship for Design of Microwave Components. His research activity involves the use of numerical techniques for modes computation of guiding structures, optimization techniques, analysis and design of waveguide slot arrays, analysis and design of patch antennas.

Luisa Deias received the Laurea degree in Electronic Engineering and Ph.D. degree in Electronic Engineering and Computer Science from the University of Cagliari, Cagliari, Italy, in 2002 and 2006, respectively. She worked as Post-Doctoral Fellow in the Electromagnetic Group at the University of Cagliari from 2006 to 2013. Her research interests include numerical techniques in electromagnetism, metamaterial analysis and optimization, microwave components and antennas analysis and design.

Giovanni Andrea Casula received the Laurea degree (summa cum laude) in Electronic Engineering and Ph.D. degree in Electronic Engineering and Computer Science from the University di Cagliari, Cagliari, Italy, in 2000 and 2004, respectively. Since March 2006, he is Assistant Professor of Electromagnetic Field and Microwave Engineering at the Dipartimento di Ingegneria Elettrica ed Elettronica, University of Cagliari. His current research interests are in the field of synthesis, analysis and design of wire, patch, and slot antennas. Casula serves as Reviewer for several international journals and is a member of the Italian Electromagnetic Society (SIEm).

Giorgio Montisci received the Laurea degree (summa cum laude) in Electronic Engineering and Ph.D. degree in Electronic Engineering and Computer Science from the University of Cagliari, Cagliari, Italy, in 1997 and 2000, respectively. Since November 2000, he is Assistant Professor of Electromagnetic Field at the Dipartimento di Ingegneria Elettrica ed Elettronica, University of Cagliari, teaching courses in electromagnetics and microwave engineering. His research activity is mainly focused on analysis and design of waveguide slot arrays, microwave holographic techniques for the diagnostic of large reflector antennas, numerical methods in electromagnetics, and printed antennas. He is author or co-author of about 40 papers in international journals and Reviewer for EM Journals.